Direct imaging of single-molecules: from dynamics of a single DNA chain to the study of complex DNA-protein interactions

BENOIT LADOUX[1], JEAN-PIERRE QUIVY[2],
PATRICK. S. DOYLE[3], GENEVIEVE ALMOUZNI[2] AND
JEAN-LOUIS VIOVY[1]

Recent years have seen significant advances in the characterization and manipulation of individual molecules. The combination of single-molecule fluorescence and micromanipulation enables one to study physical and biological systems at new length scales, to unravel qualitative mechanisms, and to measure kinetic parameters that cannot be addressed by traditional biochemistry. DNA is one of the most studied biomolecules. Imaging single DNA molecules eliminates important limitations of classical techniques and provides a new method for testing polymer dynamics and DNA–protein interactions. Here we review some applications of this new approach to physical and biological problems, focusing on videomicroscopy obser-vations of individual DNA chains extended in a shear flow. We will first describe data obtained on the stretching, relaxation and dynamics of a single tethered polymer in a shear flow, to demonstrate that the deformation of sheared tethered chains is partially governed by the thermally driven fluctuations of the chain transverse to the flow direction. Next, we will show how single-molecule videomicroscopy can be used to study in real time DNA folding into chromatin, a complex association of DNA and pro-teins responsible for the packaging of DNA in the nucleus of an eukaryotic cell.

---

[1]*Laboratoire de Physico-Chimie Curie (UMR CNRS/IC 168),* [2]*Laboratoire de Dynamique Nucléaire et Plasticité du Génome (UMR CNRS/IC 218) – Institut Curie, Section de Recherche, 26 rue d'Ulm, F-75248 PARIS cedex 05, France,* [3]*Department of Chemical Engineering, Massachusetts Institute of Technology, Cambridge, MA 02139, USA.*

Introduction to single-molecule DNA experiments

Until recently, physical and chemical studies of biological molecules were performed as averages on large populations of molecules. The development of techniques to visualize and manipulate single molecules is useful to probe heterogeneities in such an ensemble of molecules and to analyze biological reactions at the single-molecule scale. In particular, this technique has been applied extensively to DNA. DNA is a linear sequence of simple molecular subunits called nucleotides. The sequence of possible nucleotides (arginine, thymine, guanine, cytosine) carries genetic information. Single-molecule techniques, such as optical tweezers, microfibers, magnetic tweezers and atomic force microscopy, were first used to test the predictions of polymer dynamics and to study the mechanical properties of a single DNA molecule. Building on this knowledge of physical properties of DNA, micromanipulation techniques have been used for studying biological systems involving DNA replication, reparation or transcription.

Physical concepts in polymer physics

A polymer is a chain-like molecule consisting of repeating chemical sub-units referred to as monomers. Different physical models have been proposed to describe the behavior of polymer chains. A simple random walk on a discrete lattice, in which space is divided into a cubic grid of points that represent possible locations of chain monomers, and in which double occupancy of sites is not forbidden, is the simplest way of computing the statistical configurations of a polymer. This configuration is called "ideal" or "Gaussian", because the monomer density distribution follows a Gaussian law. The average coil radius of gyration R_G (a measure of the typical polymer extension in space) scales as $L^{1/2}$ where L is the end-to-end distance. In a more realistic picture, the conformation of a polymer in solution depends on the chemical structure of the monomers and on the solvent quality, which determines the nature of molecular interactions between the chain and the solvent molecules. A solvent in which the monomers favor contacts with the solvent rather than with other monomers is called a "good solvent". In such a solvent, polymers tend to expand. This so-called "excluded volume" effect implies an increase of the coil size in a good solvent with respect to the ideal coil. Such a polymer is described by a "self-avoiding" random walk in which only one monomer is allowed to occupy each lattice site. R_G then scales as $L^{3/5}$. Statistical calculations, as well as light and neutron scattering experiments have confirmed this prediction. In a poor solvent, in contrast, a polymer tends to collapse and ultimately the

collapsed chains become insoluble. The crossover between "good" solvent and "poor solvent" is called the "theta solvent", and the behavior of chains in theta solvents is that of an ideal chain.

In solution, a polymer is subject to thermal fluctuations. If a force is applied, *e.g.* to its ends, fluctuations will tend to counteract the external force and restore an end-to-end distance compatible with the largest number of configurations (maximize entropy), corresponding to a self-avoiding walk in good solvent and to a random walk in theta solvents. Several physical models have been proposed to describe the elasticity of a polymer. For a flexible chain in good solvent, the force F versus the extension has been described using scaling concepts. For small extensions, the response is linear, *i.e.* the extension is proportional to F. In the limit of large extensions, a convenient way to apply scaling theory is to divide the chain into a series of "blobs" with g monomers. Inside the blob, F is a weak perturbation, and the conformation is essentially that of a free chain of g monomers. However, the overall chain behaves as a linear string of independent blobs aligned by the force. This model predicts a linear dependence of the extension upon force, up to the limit of fully extended chain, *i.e.* when g approaches one and the chain cannot be extended any more.

For real chains, the monomers are combinations of atoms linked by chemical bonds with limited degrees of freedom, and conformation in space can not be represented directly by a random walk of chemical bonds on a lattice. An important structural parameter is the persistence length P. P corresponds to the length over which the orientational correlations between monomers in a free chain are lost. In the freely jointed chain model (FJC), the molecule is described as a sequence of rigid, independent segments connected by completely flexible joints. The flexibility is related to the number of segments per unit length and the length of a segment, b, is called the "Kuhn length" (which is twice the persistence length). The alignment by an external force is described by the Botzmann distribution. Comparing the energy associated with the action of the force on a segment b, Fb, to the thermal energy kT (where k is the Botzmann constant and T the temperature), the relative extension $<R>/L$ of the chain is given by: $<R>/L = L_g (Fb/kT)$ where L_g is the Langevin function, $<R>$ is the average end-to-end separation and L is the contour length. When the links between monomers are rather flexible, such as for polystyrene, this model describes relatively well the conformation and elasticity of the polymer.

However, many polymers (such as double stranded DNA) do not have flexible bonds between individual monomers, and a better

representation is a continuous flexible rod which has a length *L* and curves smoothly as a result of thermal fluctuations. A polymer is called "semiflexible" if *P* is much larger than the monomer size, but smaller than the total curvilinear length *L*. For this class of polymers, the linear regime in the force/extension curves is more limited and it becomes important to take into account the continuous nature of chain bending for higher tensions. This kind of polymer can be described by a "worm-like" chain model (WLC) which differs from the FJC model in that it contains a term associated with chain bending. Starting at an arbitrary location on the chain, the chain's local direction decorrelates at a distance *s* along the chain contour according to exp(–*s/P*). The mean extension for a given external force can be calculated using Botzmann's law. A good approximation to the relation between force and chain extension was proposed by Marko and Siggia[1] (equation (1)):

$$\frac{FP}{kT} = \frac{1}{4}\left(1 - \frac{R}{L}\right)^{-2} - \frac{1}{4} + \frac{R}{L} \qquad (1)$$

Extension experiments have shown that DNA molecules are well described by the WLC model.

Visualizing and manipulating single DNA molecules

Observations of individual DNA chains by fluorescence videomicroscopy have provided detailed information about polymer dynamics, revealed surprising phenomena, allowed testing of polymer models (such as Zimm or Rouse models) and development of new ones. Duplex DNA molecules have a persistence length of approximately 50nm and a diameter of 2nm. In the size-range which can be manipulated as single molecules, *L/P* is >>1 and aqueous solutions are a good solvent.

DNA present several experimental advantages over other polymers for micromanipulation: the length of the molecules is perfectly known (most single DNA experiments use λ-bacteriophage DNA which consists of 48,502 base pairs giving a curvilinear length of 16.3 μm), samples containing molecules from the same type of phage are inherently monodisperse and molecular biology offers a large range of possibilities for staining, cutting and functionalizing the molecules.

Relaxation

Steve Chu's group at Stanford University has done considerable work based on visualization and micromanipulation of single DNA

molecules in various hydrodynamic flows to test polymer theories. First, this group studied the relaxation of single polymers starting from near complete extension[2]. Manipulating a small bead attached to a single DNA molecule with an optical tweezer in a uniform flow, they determined the longest relaxation time τ as a function of length and found the following simple scaling law: $\tau \sim L^{1.66}$. Surprisingly, the exponent is closer to the one predicted by the Zimm model (which includes hydrodynamic interactions within the chain in the dynamics equations) than to the prediction of the Rouse model (which does not take into account intramolecular interactions). As a matter of fact, one would expect that hydrodynamic interactions would be negligible for extended chains, *i.e.* the chain would be "free-draining", since at high extension different sections of the chain are unlikely to be in close proximity. Manneville *et al.* measured the relaxation of single DNA molecule extended in shearing flow[3]. They analyzed the recoil of DNA and compared their results to the "stem and flower" model proposed by Brochard *et al.*[4]. This model is a refinement of the "blob" theory, taking into account the possibility of "blobs" of different sizes, if external forces are distributed along the chain, and not applied only at the end. This model distinguishes several regimes according to the flow strengths. Under weak flows, the polymer is a weakly deformed statistical coil. At large deformations the chain is represented as a fully stretched part (the stem) terminated by a blob (the flower). Increasing the flow further, the flower disappears to give a completely straight molecule. The results by Manneville *et al.* agreed with the predictions of the "stem and flower" model, showing that the relaxation follows a universal scaling with time, $L–R(t) \sim t^{0.51}$ where $R(t)$ is the extension at time t.

Stretching

The deformation of single DNA molecules in different types of steady flows has been studied by Chu's group. The stretching of a tethered DNA molecule in a uniform fluid flow provided information on the hydrodynamic coupling between the polymer and the fluid. The results show that very large chains must be used in order to enter a regime where scaling laws for hydrodynamic interactions can be applied[5]. The stretching of free chains in elongational flow revealed complex, diverse dynamics depending upon the initial configuration of the chains[6,7] and enabled observation of the coil-stretch transition at a critical velocity gradient. Free molecules in shear flow displayed large, aperiodic temporal fluctuations corresponding to an end-to-end tumbling of the molecule. These examples demonstrate that individual DNA chains in an ensemble can behave very differ-

ently from each other. Studying physical properties at the single-molecule level could eliminate many of the ambiguities associated with classical bulk experiments which average over a huge number of molecules.

Stretching DNA beyond the entropic regime

Other experiments were performed in several laboratories in order to study the elasticity of DNA, using different techniques, such as magnetic beads[8,9], glass needles[10], and optical traps[11]. In these experiments, one end of the DNA molecule is attached to a fixed surface by a specific chemical reaction, and the other end is attached to a mobile object (bead, fiber), in order to stretch the molecule. These experiments unveiled different force/extension regimes for double-stranded DNA (dsDNA). The first "entropic" elasticity regime, up to 10 pN, is well described by the WLC model. Above 10 pN, the response deviates from the prediction of the WLC model because of deformation of the chemical bonds themselves. For forces around 65 pN or more, an abrupt transition occurs, stretching the DNA up to 70% beyond its natural contour length[10,11]. This overstretching transition corresponds to a plateau in the force/extension curve and is attributed to a structural transition into a "stretched" structure called "S-DNA" in which the double helix itself is completely rearranged, and stacking interactions between the bases are deeply affected.

DNA–protein interactions

It is becoming more and more clear that mechanical properties of DNA are essential to its biological functions and single-molecule experiments are now used to test biological systems by applying forces on DNA-protein structures. For instance, the DNA overstretching ratio observed in the mechanically overstretched state is very close to the 1.5 times extension of DNA observed when DNA is bound to recA, a bacterial protein involved in homologous recombination and repair of DNA. This protein is essential for the conservation and evolution of the genome. The mechanics of recA-DNA filaments has been studied in several laboratories[12–14]. Other experiments investigate replication and transcription systems by analyzing properties of polymerases or topoisomerases on single DNA molecule[15–18]. Recently, Bustamante's group studied chromatin by stretching and relaxing single chromatin fibers (isolated from chicken erythrocytes) with optical tweezers[19].

Experimental set-up

In this section, we present in more detail the methods used and some results obtained in our laboratory in the field of single molecules. Our experimental system is based on the attachment of single DNA molecules by one end to the bottom of a rectangular microchannel. These tethered DNA molecules were submitted to shear flow and their behavior vizualized in real time using fluorescence microscopy techniques. Using this method we studied the dynamics of tethered chains and chromatin assembly on single molecules.

DNA biochemical modifications and surface treatment

We used standard biotin-streptavidin biochemical reactions to attach DNA molecules on the surface. A biotinylated oligonucleotide was ligated to the end of the λ-phage DNA. In order to build longer molecules, λ-phage DNA molecules can be attached to each other by their complementary dangling single-chain ends (12 bp), in order to make concatemers. DNA molecules were then attached onto microscope coverslips covered by streptavidin. The non-covalent biotin–streptavidin bond provides a tight association ($kd \approx 10^{-15}M^{-1}$).

Staining and solutions

Imaging single DNA molecules requires fluorescent dyes with a high quantum yield and a low background. We used a standard dye (YOYO-1, Molecular Probes, excitation and emission wavelengths are respectively 491nm and 509nm) to fluorescently label DNA. The intercalation alters the local structure of DNA and increases its contour length. At the staining ratios used here (one dye molecule per eight or ten base pairs, depending on the experiment), we estimated that the contour lengths of λ DNA increased from 16.2 μm to 18 or 18.9 μm, respectively.
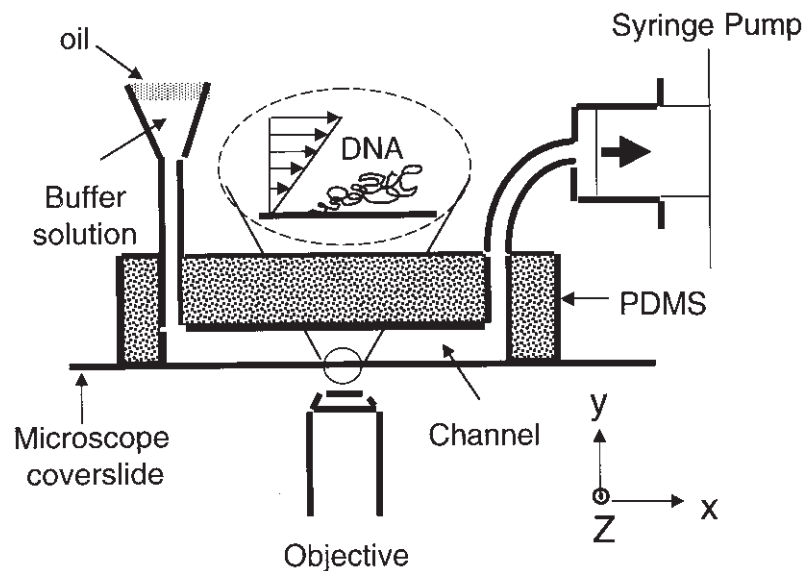
In water or conventional buffers, dyes rapidly photobleach, and can lead to DNA photoscission when intercalated. Thus, to observe a single molecule for a long time we needed to optimize the signal over noise ratio and have a solution which minimizes the photobleaching. The presence of oxygen radicals is one of the main causes of photobleaching and photoscission. The presence of singlet oxygen was minimized by adding to the solution 2% β-mercaptoethanol. In addition, dissolved oxygen was reduced by the use of glucose oxydase and catalase, in the presence of glucose. When combining these approaches, a single molecule could typically be observed for a period of 10 min.

Videomicroscopy technique and analysis

We imaged single DNA molecules using video enhanced fluorescence microscopy (Figure 1). Stained DNA were excited with an argon-ion laser (Innova 70, Coherent) and visualized using a cooled intensified CCD camera (Lhesa, les Ulis, France). The images were converted to digital format, transferred to a computer and the visual length of the molecules was determined using custom-programmed software. For a sequence of images, the program automatically subtracted off the background fluorescence and then determined the positions of non-zero pixels (zero corresponding to no fluorescence and hence no DNA). The visual length of the DNA was defined as the difference in the x coordinates of the beginning and ending fluorescence in an image.

Microchannel preparation

A poly(dimethylsiloxane) (PDMS) elastomer flow channel (a few hundred micrometers in width, between 100 and 200 μm in height, depending on the experiments, and 2.5 cm in length) was prepared on a microscope coverslip coated with streptavidin. We used soft lithography[20] to fabricate the channel. The PDMS is cast over a template prepared by photolithography. The elastic and hydrophobic properties of PDMS allow its release from the template, and adhesion to glass surfaces. Thus, a channel is formed by pressing the cast

Fig. 1 *Experimental setup.*

PDMS onto a biotinylated coverslide. DNA molecules were introduced into the channel and attached by one end to the biotins at the surface. A controlled flow is then applied in the channel using a syringe pump (Figure 1). This circulating system also allows us to introduce biological samples into the channel, in order to observe their interactions with the grafted DNA molecules.
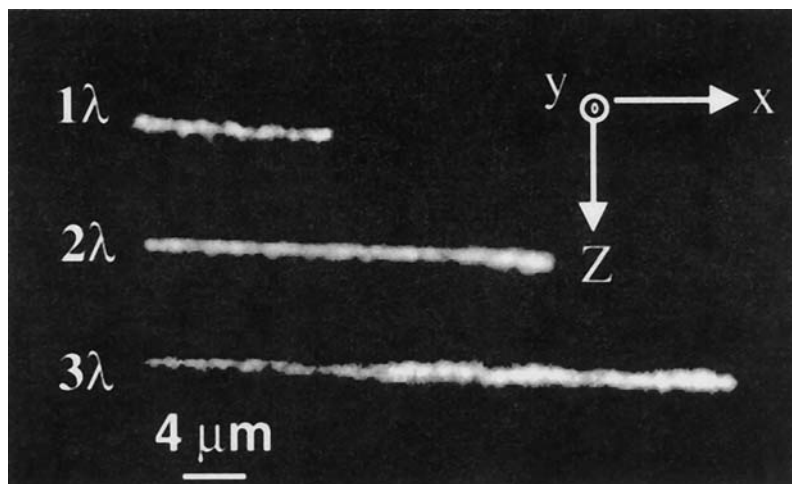
Stretching of tethered DNA chains

Introduction

The deformation of polymers tethered to surfaces is of central interest in many practical applications such as colloidal stabilization, capillary electrophoresis, lubrication, chromatography, biocompatibility, or for biological membranes in which long molecules constituting the extracellular matrix protrude far beyond the phospholipid bilayer. We have already mentioned that various experiments[2,3,6,7] have been dedicated to the study of single DNA chain behavior subject to different hydrodynamic flows. The behavior of a chain near to a wall, however, had not been investigated by this technique. The dynamics of sheared polymers is nontrivial due to both a rotational and extensional component to the flow. Theoretical and numerical work dealing with the shearing of tethered polymers has focused mostly on an average representation of the chains. Studying polymer physics at the single-molecule level appeared as an important step to provide new information compared with the simplified mental representation of an "average random coil".

Relaxation of a single tethered polymer

We studied the relaxation time of single DNA molecules as a function of their length. The fundamental relaxation time τ was obtained either by fitting the decay of the autocorrelation function $<R(t)R(t+T)>$ at equilibrium (no flow) to a single exponential (R is the chain extension, t is the time and T is the delay time), or by stretching the chains at a moderate shear rate $\dot{\gamma}$, stopping the flow and measuring the relaxation of the chain back to its equilibrium coiled configuration.

We measured the relaxation time of chains after stretching for several multimers of λ-DNA lengths (λ, 2λ, 3λ. having contour lengths L of 18.9 μm, 37.8 μm and 56.7 μm, respectively, see Figure 2). For each contour length, the curves correspond to averages over a population of 15 chains. After the chains have relaxed to 1/3 L, the relaxation is dominated by the slowest mode and the plot of $R^2(t)$ versus t is well described by a single exponential. The relation

Fig. 2 *Sample DNA configurations for various lengths. The flow is in the positive direction and the images are in the x-z plane (from ref. 20).*

between the visual length, $R(t)$, and the relaxation time τ is the following: $<R(t)R(t)>=c_1 \exp(-t/\tau) + c_2$. where c_1, τ and c_2 are free parameters. We determined in this case $\tau_\lambda = 0.45$s, $\tau_{2\lambda} = 1.45$s and $\tau_{3\lambda} = 2.56$s. The scaling of the relaxation time as a function of the contour length of the chain follows: $\tau \propto L^{1.59}$. The scaling exponent is closer to the one predicted by the Zimm model, in which hydrodynamic coupling within the chain is included (the predicted exponent is either 1.5 or 1.8 depending on the solvent conditions), than to that predicted by the Rouse model (the predicted exponent is 2), which neglects such intrachain hydrodynamics.

Stretching of a chain subject to shear flow as a function of length

We studied the deformation of a single DNA chain as a function of the shear rate. Stretching a single chain in a shear flow has been theoretically studied[5] using the "stem and flower" model. As for a uniform flow, the authors used a blob model, which does not take into account the nonlinear elasticity of the molecule. At large shear rates the molecule is divided into two parts, the "stem", in which the chain is fully stretched, and the "flower" containing a series of blobs. In the following, we compare experimental and numerical results to theoretical predictions[21].

First we define a dimensionless parameter $Wi = \dot{\gamma}\tau$, the Weissenberg number, which characterizes the flow strength. It is

expected that large deformations of a tethered polymer will occur when the flow distorts the polymer faster than it can naturally relax back to the equilibrium coiled configuration, *i.e.* for $Wi > 1$.

From videomicroscopy images, the mean fractional chain extension $<R>/L$ is obtained using averages over several molecules. A single curve could describe the mean fractional chain extension versus Wi for all the different lengths of the molecules (see ref. 21). Figure 3 represents an example of the mean fractionnal extension versus Wi for the monomer of λ-DNA. Two parts are apparent in the curve: the first one corresponds to a rapid increase of $<R>/L$ with Wi up to $Wi \sim 20$ and the second one to a very slowly approach to full extension.

To gain further insight into the approach to full extension, we compared these experimental results with numerical simulations and with scaling laws derived from the different theoretical models mentioned above: the FJC model, the WLC model and the "stem and flower" model[21]. To develop scaling theories, a further approximation is required: we assumed that a stretched chain is free-draining
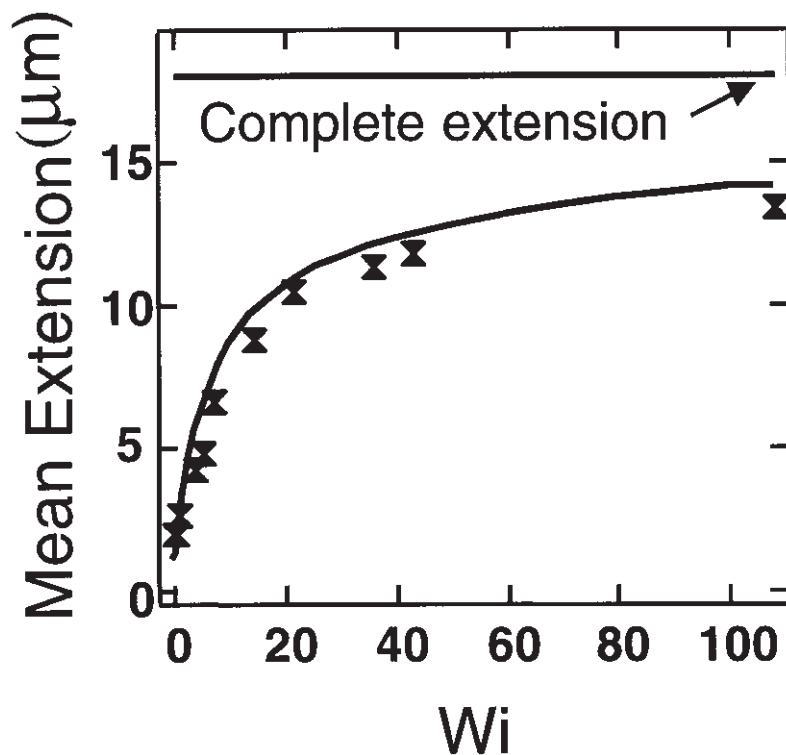

Fig. 3 Schematic of a tethered chain (from ref. 20).

and that tension is uniform along the chain. The width of a tethered chain (Figure 4) in the y direction is determined by the transverse thermal fluctuations δy. This average lateral extension determines flow velocities sampled (as the velocity increases linearly from the surface) and hence the hydrodynamic force exerted on the chain in the x direction. First, we can relate the transverse fluctuations to the spring force, F, required to maintain the ends of the chain at a given distance, R, using an effective transverse spring constant: $1/2\ F(R)/R\ \delta y = kT$. Then the balance of the spring force and the hydrodynamic force yields the extension of the chain ($F = \zeta\dot{\gamma}\ \delta y$ where ζ is the drag coefficient). Combining these equations with the analytic expression for the chosen spring force model leads to:
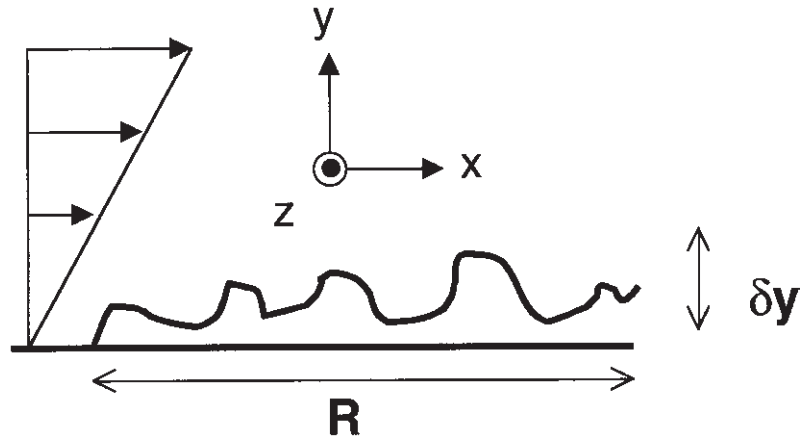
$$\epsilon \propto \dot{\gamma}^{-1/3} \qquad \text{for the WLC model} \tag{2}$$

$$\epsilon \propto \dot{\gamma}^{-2/3} \qquad \text{for the FJC model} \tag{3}$$

$$\epsilon \propto \dot{\gamma}^{-1} \qquad \text{for the Stem and Flower model} \tag{4}$$

where is ϵ defined as $\epsilon = 1 - R/L$.

We also performed numerical simulations based on Brownian dynamics simulations[22] of a bead-spring chain model. A chain consisting of beads connected by springs with *WLC* elasticity is used to simulate DNA molecule. The parameters in the model have been calculated *a priori* using independently measured molecular parameters. The simulations neglect hydrodynamic interactions, viscous

Fig. 4 *Mean fractional chain extension for a λ-phage DNA versus Wi. The line is the result of simulations and the symbols are experimental data.*

drag is exerted on the beads only and a short-ranged repulsive potential simulates the surface where the molecule is attached. Good agreement was found between experiments and simulations for the curves of the mean extension versus *Wi* (Figure 3).
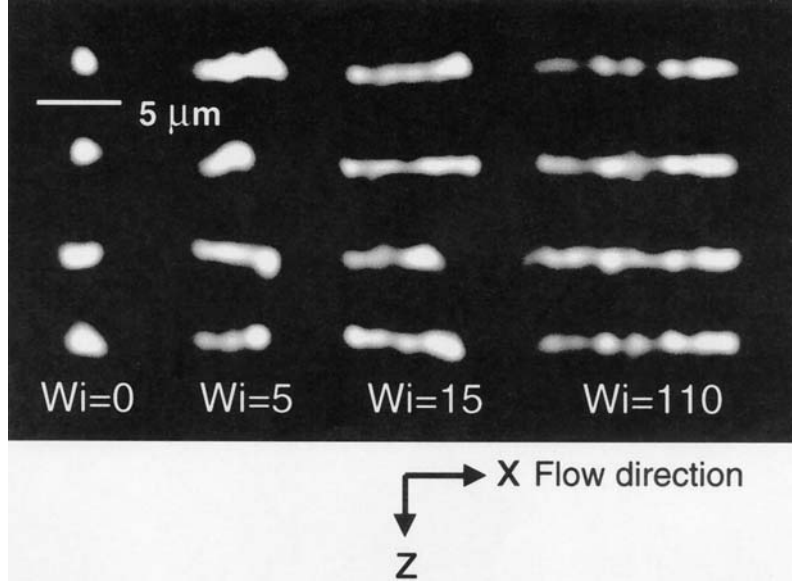
Comparison between both experimental curves and simulations of the mean extension to the scaling laws shows that experimental and simulation data follow the scaling law derived for the *WLC* (equation (2)). This analysis demonstrates that a nonlinear elastic force law is necessary to describe the extension of DNA at high shear rates and that transverse fluctuations play a key role in explaining the deformations.

Dynamics of a tethered polymer in shear flow

In this section we present a study of the dynamics of a single polymer tethered to a solid surface, confirming the important role played by thermal fluctuations and the interest of single-molecule experiments. We already mentioned that a shear flow has both an extensional and rotational component, responsible for the tumbling in the shearing of free DNA. However, in the case of tethered chains, the surface frustrates the tumbling motion. What could be the dynamics in such an experimental system?

We determined the polymer chain extension as a function of time in a large range of shear rates and measured the temporal fluctuations of the length of the chain. These observations unveiled an unexpected phenomenon[23]. In Figure 5, we show an example of the configurations of DNA as a function of time for four different shear rates: fluctuations are weak at both small and large *Wi*, and large at intermediate *Wi*. The determination of the standard deviation σ of the temporal chain extension (Figure 6) clearly indicates two different regimes: it first increases up to a maximum value of $Wi = 5.1$, then decreases with increasing *Wi*. The most intuitive approach, a mean-field approach, would consider the molecule as trapped in a potential well with the fluctuations driven by thermal motion. Then one would have expected a monotonic decrease in the amplitude of the fluctuations: the more the molecule is stretched, the less it fluctuates. Indeed, this behavior has been observed in the fluctuations of DNA molecules stretched by a homogeneous plug flow[24]. It seems, then, that the mean field approach fails in our case.

Trying to explain this phenomenon has leaded us to consider a simpler model: a Hookean spring attached at one end to a surface and at the other end to a Brownian bead subject to shear flow. For such a system, the force law is linear in chain extension. Equations of motion are the following (neglecting the inertial term):
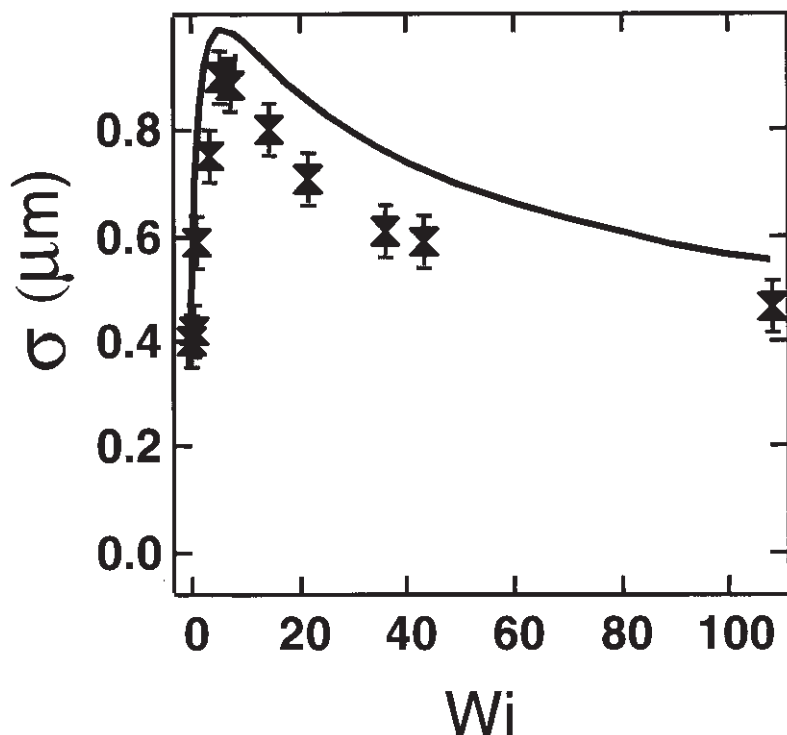
Fig. 5 *Time series (top to bottom) of the configurations of single DNA molecules at varying flow strengths. In each series the images are separated by an interval of 0.4s (from ref. 22).*

$$\frac{\mathrm{d}x}{\mathrm{d}t} = kx / \zeta + \dot{\gamma}y + f_{bx}(t) / \zeta \qquad (5)$$

$$\frac{\mathrm{d}y}{\mathrm{d}t} = ky / \zeta + f_{by}(t) / \zeta \qquad (6)$$

where k, ζ, and f_b are the spring constant, the friction coefficient of the bead and the Brownian force (*i.e.* $<f_{bi}(t)f_{bi}(t')>=2k_BT\delta(t-t')$ where k_B is the Boltzmann constant), respectively. The equation of motion in the y direction is that of a bead submitted to Brownian motion in a harmonic well. In the x direction, forces derive from the Brownian motion, the elastic spring and a third term corresponding to a contribution from the flow velocity. The mean square deviation $<x(t)-x(0)>^2$ contains two terms: the first one corresponding to the standard deviation of a bead in a harmonic well, and another contribution, arising from the coupling between the shear rate and the transverse fluctuations in the y direction. This means that at very small flow strengths the dynamics are dominated by the thermal motions in all directions. At larger flow strengths the temporal fluctuations in the x direction are mostly due to the transverse Brownian fluctuations
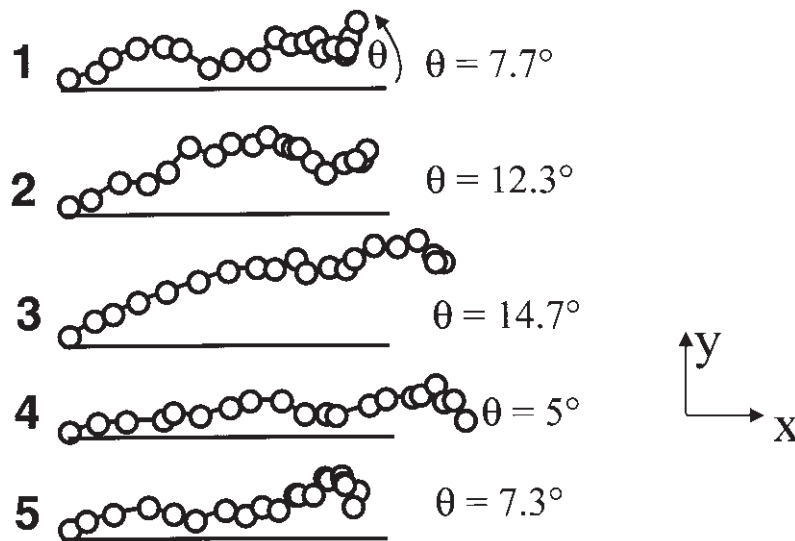
Fig. 6 *Standard deviation σ of the temporal chain extension versus Wi. The line is the result of simulations and the symbols are experimental data.*

which become amplified by the shear flow. In this regime the extension probability distribution function becomes broader with increasing *Wi*. This coupling explains the observed shear enhanced fluctuations. This phenomenon is analogous to that described by Taylor, for the dispersion of colloidal suspensions under shear flow[25]. In this case the mean square deviation is $<x(t)-x(0)>^2 = Dt + D_1\dot{\gamma}^2t^3$ where D and D_1 are constant parameters. The first term is due to the simple diffusion and the second one is due to the coupling between the shear flow and the transverse fluctuations, leading to the experimentally observed shear enhanced dispersion of Brownian suspensions.

Real polymers, however, cannot be described quantitatively by a simple model with a single bead and a single spring. In particular, the behavior we observe at high shear rates diverge from the above "Taylor like" enhanced fluctuations. To get a more realistic description, we used Brownian dynamics simulations of a bead-spring chain model with *WLC* elasticity, as described before. Strong qualitative and quantitative agreement between the simulations and experi-

ments is found (Figure 6). We have distinguished two regimes in the amplitude of fluctuations *versus Wi*. The first one is observed for small extensions of the chain, when the elasticity is still linear. The second one, where the amplitude of the fluctuations decrease with increasing *Wi*, is due to nonlinear elasticity of the chain at large deformations. The simulations allow us to clearly follow not only the chain ends, but also the dynamics of the chain in the vorticity plane (perpendicular to the plane of focus in the experiments). Observing the dynamics of the simulated polymers we found that they describe a continuous recirculating motion or *cyclic dynamics* (Figure 7). A chain, initially in a compact configuration near the interface, experiences a fluctuation perpendicular to the surface and stretches quickly to a more extended state. This extended polymer will slowly rotate towards the interface and retract at the same time, until it experiences another substantial fluctuation perpendicular to the surface which reinitializes the cycle. Thus the recirculating motion in the vorticity plane is responsible for the observed length fluctuations in the flow direction.

We have presented experimental data on the dynamics of a dilute sheared polymer brush. Simulations where used to formulate a mechanism to explain the shear enhanced fluctuations. The current study revealed the *cyclic dynamics* of the dilute polymer brush. The

Fig. 7 *Results from simulations for Wi =5.1. Cyclic chain dynamics. The angle θ is the orientation of the vector joining the tethering point to the center of mass of the chain, with regard to the tethering surface (from ref. 22).*

conformation and the dynamics of a sheared tethered polymer are dominated by fluctuations at most *Wi*. A standard mean field approach cannot capture these complex dynamics. Furthermore, we show that a tethered sheared chain is a rather unique dynamical system and that the single-molecule approach is a powerful method to observe and analyze these dynamics. The understanding of the physical properties of a single DNA chain stretched by a shear flow leads us to use this system to observe DNA–protein interactions and in particular, chromatin assembly.

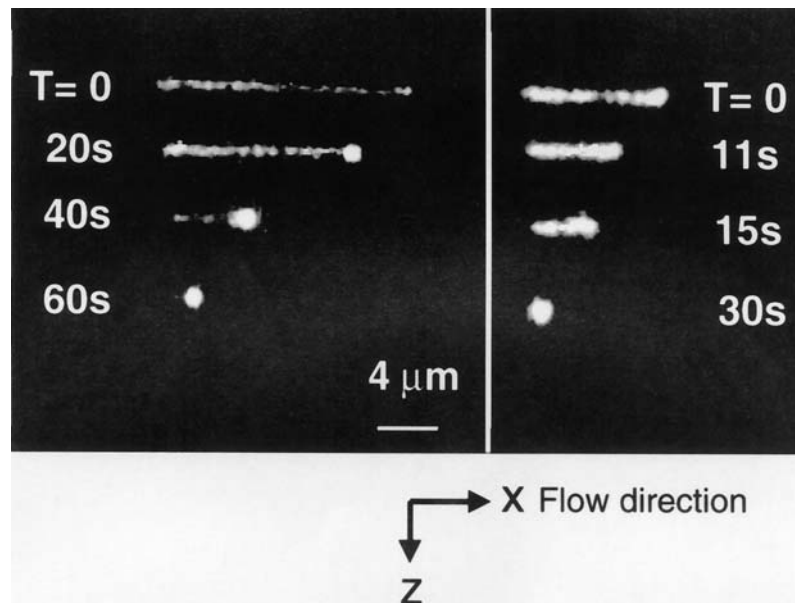## Using single-molecule to study biological process such as chromatin assembly

Until now, we considered DNA only as a model polymer, but this polymer is of course a very unique and important component of life. DNA is the support of genetic information. *In vivo*, DNA is located in the nucleus of eucaryotic cells. It is not present as a naked molecule, but as chromatin. Chromatin is composed of a repetitive fundamental structure – the nucleosome[26], that results from the wrapping of the DNA around a histone octamer[27] (one H3–H4 tetramer and two H2A–H2B dimers). This organization induces a first level of compaction into the so-called 10 nm nucleofilament or "beads on a string" structure. Further higher levels of compaction are achieved (such as the 30 nm fiber) to reach the highest level of compaction into metaphasic chromosomes[27,28]. The organization of DNA into chromatin allows the packaging of the considerable length of the genomic DNA into the cell nucleus (the human genome reaches lengths of several hundreds of centimeters and the typical size of cell nucleus is about 2 μm). It is important for this structure to remain dynamic in order to allow DNA metabolic processes such as reparation, recombination, transcription and replication to occur. These functions are linked to important rearrangements of the chromatin structure, associated with local assembly and disassembly of the organization. Therefore, studying the process of chromatin and nucleosome assembly is of special importance in order to understand how the dynamics of chromatin structure can regulate DNA metabolism.

We used fluorescence microscopy applied to single DNA molecules, in order to study in real time the early events of chromatin assembly[29]. The experimental set-up is the same as the one described in the section "Experimental set-up".

Various biological systems have been used to study nucleosome assembly, such as purified histones, *in vitro* cell-free systems derived

from *Xenopus* eggs, *Drosophilia embryos*, or cultured cells. In the following, we describe a study of chromatin assembly on individual DNA molecules, in a cell-free system derived from *Xenopus* eggs and competent for physiological chromatin assembly[30].

The shear flow induced in PDMS channel is used to stretch DNA molecules and thereafter *Xenopus* egg extracts are introduced at various dilutions. Videomicroscopy enabled us to follow in real time the compaction of DNA molecules induced by these extracts (Figure 8). The compaction from the stretched state of DNA to the compacted one at the anchored end of the molecule is fast (complete retraction at the level of optical resolution occurs in less than one minute in our conditions). Such a rapid compaction rate was unexpected, since conventional enzymatic assays based, *e.g.* on partial digestion of DNA, reveal chromatin structure on a time-scale of several tens of minutes. We performed various complementary experiments to confirm the relevance of our experiments to chromatin condensation, and to gain further insight into molecular mechanisms. First, a 0.1% SDS solution led to a recovery of the intact initial length of the naked DNA. Second, we used different extracts
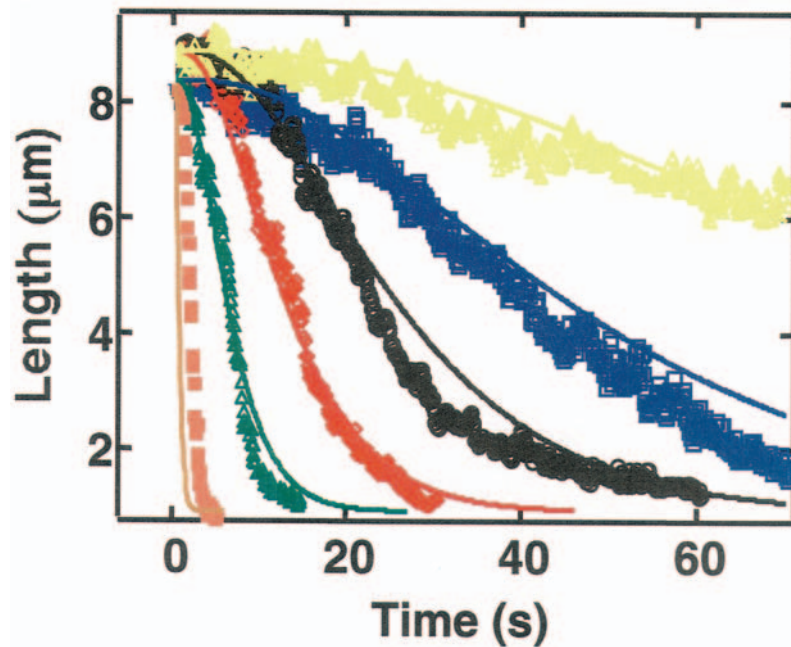

Fig. 8 *Examples of compaction of individual DNA molecules with time in the presence of 1:50 diluted extracts at shear rates of 26.25 s⁻¹ (left) and 1050 s⁻¹ (right) (from ref. 28, Copyright 2000 National Academy of Sciences, USA).*

known for their ability (such as *Drosophila* embryo extracts DREX) or inability (such as *Drosophila* nuclear extracts TRAX) to assemble chromatin. In the first case a similar compaction was observed while no compaction of the DNA was detected in the second. Third, we confirmed that the DNA compaction is dependent on the presence of histones: no compaction was obtained when using extracts whose chromatin assembly capacity and histones are initially titrated out, and DNA compaction was recovered when these titrated extracts are complemented with purified histones.

We also studied quantitatively the influence of several experimental parameters, such as the flow strength and the dilution factor of the extracts, on the compaction. The compaction was affected by shear rates stronger than 175 s^{-1}. At 1,050 s^{-1} the compaction curve (DNA length as a function of time) showed a behavior qualitatively different from compaction at lower shear rates. First, nucleation of the compaction clearly initiated at the free end of the molecule (Figure 8, left) while it seemed to be distributed all along the molecule for lower shear flows (Figure 8, right). Second, compaction was slower at 1,050 s^{-1} than at lower shear rates (26.25 s^{-1} and 175 s^{-1}). How does tension on the DNA influence the compaction? In our experiments, chain tension is due to drag forces, and it varies all along the chain, from a zero tension at the free end to a maximal tension at the anchored end. The numerical simulations described in section *"Stretching of tethered chains"* (see also ref. 22), provided an evaluation of the maximum tension at the attachment point: 0.3, 2 and 12 pN for shear rates of 26.25, 175 and 1,050 s^{-1}, respectively. Forces of the order of pN can affect significantly the assembly process. Recent experiments[18] studied the stretching and relaxation of chicken erythrocyte chromatin fibers with laser tweezers : at low forces (under 8 pN), force/extension curves are reversible and display a plateau attributed to internucleosomal attraction forces at 6 pN. At higher forces (> 20 pN), a hysteresis appears, due to the dissociation of nucleosomal core particles from the DNA. This comparison suggests that the forces realized in our experiments of DNA compaction are of the same order as those required to destabilize an already organized chromatin structure.

To avoid the complications due to the action of external forces, we have studied the compaction at flow rates at which compaction rates are independent from the chain tension. Figure 9 represents the compaction at a shear rate of 26.25 s^{-1} for several dilutions of the extracts. Data are obtained by averaging over a large number of molecules to improve signal to noise ratio, but the compaction of an individual molecule presents an identical kinetic process[29] as the
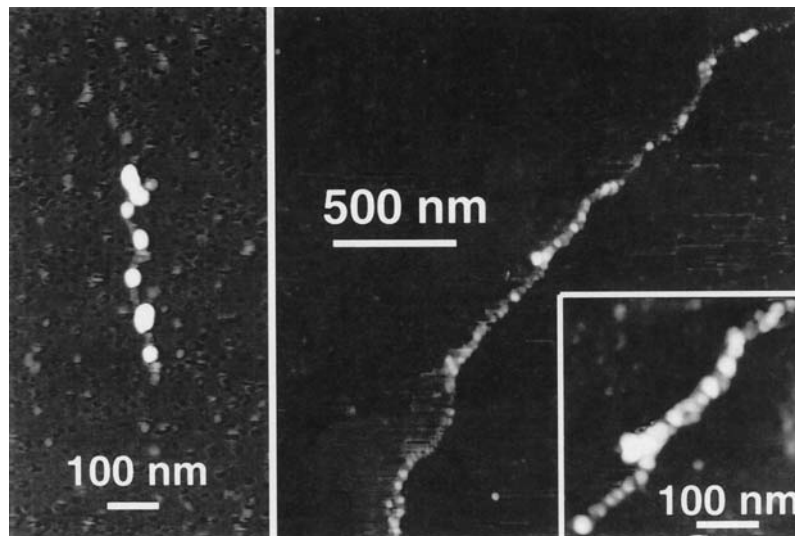
Fig. 9 *Length versus elapsed time. For different extract dilutions at a shear rate 26.25 s-1: 1:2.5 (■ orange); 1:25 (△ green); 1:50 (◇ red); 1:100 (○ black); 1:200 (□ blue); 1:400 (△ yellow). Points represent experimental data, and lines were fitted using a 3-step model. Different extracts yielded compaction profiles identical within experimental error (from ref. 28, Copyright 2000 National Academy of Sciences, U.S.A.).*

averaged curve. First the curves present a lag time period, defined as the time of intercept of the tangent to inflexion point with the horizontal line drawn from length at time 0. Then the compaction rate achieves its maximal value. The lag time and the compaction rate vary linearly with the dilution factor of the extracts[29]. In comparison, purified histones prebound to polyglutamic acid[31] also led to compaction, but a rather different kinetic law was followed (quasi-exponential) and the rate was at least ten times slower than the one with *Xenopus* egg extracts. These differences can be attributed to the presence of dedicated chromatin assembly factors and the existence of multiple assembly pathways operating within the extract.

The above set of data provide strong evidence that the compaction observed was related to chromatin assembly (only extracts competent for chromatin assembly induce a compaction, compaction is dependent on the presence of histones and corresponds to a packing ratio of DNA compatible with chromatin structures). In addition we

performed scanning force microscopy SFM experiments on DNA incubated 1 minute with cell extracts in conditions similar to those used in the videomicroscopy experiments (in these conditions, full compaction at the resolution of the optical microscope is obtained after one minute). SFM was used in tapping mode in air to avoid potential damages of the surface. Examples of the resulting fibers are represented in Figure 10. They present strong similarities with those obtained for native chromatin[32] such as the "beads-on-a-string" structures. With less diluted extracts, more compact structures, reminiscent of the 30-nm fiber, were obtained. These observations confirm that chromatin assembly can be achieved on very short time scales.

Finally our results provide detailed information about the kinetic pathway followed by the nucleosome assembly. The sigmoidal length decrease (Figure 9) indicates that early chromatin assembly involve several steps with comparable time scales. A kinetic model with a minimum of three steps was necessary to fit our compaction curves. Previous *in vitro* and *in vivo* data indicated a two-step model

Fig. 10 *SFM images of the assembled chromatin (at 50% humidity in tapping mode on a Nanoscope III (Digital Instruments Inc.)) after 1 min incubation. (Left) Short lambda-phage DNA fragment in extract at 1:100 dilution. (Right) T4 DNA in extract at 1:25 dilution (insert: magnified view). A drop was diluted in a large amount of buffer, immediately deposited on mica, incubated 20 s to initiate adsorption of complexes, and spread using argon to favor an extended conformation (from ref. 28, Copyright 2000 National academy of Sciences, U.S.A.).*

for the nucleosome formation: tetramers of histones H3 and H4 are deposited first on the DNA and in a subsequent step, dimers histones H2A and H2B are added to form the complete nucleosomal core particle. To integrate all these findings, we propose the following pathway:

(1) a H3–H4 tetramer is deposited at a random position along the DNA
(2) a first H2A–H2B dimer binds on one of two available sites on the $(H3–H4)_2$/DNA complex
(3) a second H2A–H2B dimer binds on the remaining site
(4) DNA wraps around the complex, leading to the formation of the nucleosomal particle.

This model allows a direct measure of the kinetic parameters of the reaction. Deducing the histone concentration from the dilution factor of the extracts, we used the same kinetic constants to fit all the data (Figure 9). The reaction constants of the first three steps are of the same order of magnitude, and the constant of the last step must be much larger than the others, in order to obtain an adequate fit. Our model implies that DNA wrapping is the last step in this early series of events.

This scheme receives further evidence from the fact that an enrichment in H2A-H2B in the extracts, speeds up the reaction in quantitative agreement with the kinetic equation, confirming that H2A-H2B binding is a limiting step[29].

Conclusion

Single-DNA molecule experiments can be useful to investigate very diverse problems, ranging from polymer dynamics to DNA-protein interactions. In this article, we reviewed a few applications of this approach, using a unique experimental set-up. From a physicist's point of view, single-molecule experiments are helpful to understand how the behavior of individual molecules can account for macroscopic behavior. In numerous cases, in particular for macromolecules with a high number of degrees of freedom and nonlinear behavior, fluctuations can be large, and lead to surprising phenomenon. The study of a single tethered DNA chain subject to shear flow has unveiled unexpected cyclic dynamics and has shed new light on this physical problem. These experiments provide a new approach for the study of biological processes. Studying chromatin assembly at the level of single-molecule and in real time has provided definite

information about kinetics, time scales and forces involved in this process. These two examples, together with the considerable work in the field performed by other groups, and reviewed in the first part of this article, demonstrate the importance of the new type of information that can be obtained from single-molecule experiments.

References

1. Marko, J.F. & Siggia, E. D. (1995) Stretching DNA. *Macromolecules*, **28** , 8759.
2. Perkins, T.T., Quake, S.R., Smith, D.E. & Chu, S. (1994) Relaxation of a single DNA molecule observed by optical microscopy. *Science*, **264**, 822.
3. Manneville, S., Cluzel, P., Viovy, J.-L., Chatenay, D. & Caron, F. (1996) Evidence for the universal scaling behaviour of a freely relaxing DNA molecule. *Europhys. Lett.*, **36,** 413.
4. Brochard, F. (1993) Deformations of one tethered chain in strong flows. *Europhys. Lett.*, **23**, 105.
5. Larson, R.G., Perkins, T.T., Smith, D. E. & Chu, S. (1997) Hydrodynamics of a DNA molecule in a flow field. *Phys. Rev. E.*, **55**, 1794.
6. Perkins, T. T., Smith, D. E. & Chu, S. (1997) Single polymer dynamics in an elongational flow. *Science*, **276**, 2026.
7. Smith, D. E. & Chu, S. (1998) Response of flexible polymers to a sudden elongational flow. *Science*, **281**, 1335.
8. Smith, S. B., Finzi, L & Bustamante, C. (1992) Direct mechanical measurement of the elasticity of single DNA molecules by using magnetic beads. *Science*, **258**, 1122.
9. Strick, T. R., Allemand, J-F., Bensimon, D., Bensimon, A. & Croquette, V. (1996) The elasticity of a single supercoiled DNA molecule. *Science*, **271**, 1835.
10. Cluzel, P., Lebrun, A., Heller, C., Lavery, R., Viovy, J-L., Chatenay, D. & Caron, F. (1996) DNA†: an extensible molecule. *Science*, **271**, 792.
11. Smith, S. B., Cui, Y.& Bustamante, C. (1996) Overstretching B-DNA: the elastic response of individual double-stranded and single-stranded DNA molecules. *Science*, **271**, 795.
12. Léger, J-F., Robert, J., Bourdieu, L., Chatenay, D. & Marko, J. (1998) RecA binding to a single double-stranded DNA molecule: a possible role of DNA conformational fluctuations. *Proc. Natl. Acad. Sci.*, **95**, 12295.
13. Shivashankar, G. V., Feingold, M., Krichevsky, O. & Libchaber, A. (1999) RecA polymerisation on double-stranded DNA by using single-molecule manipulation†: the role of ATP hydrolysis. *Proc. Natl. Acad. Sci.*, **96**, 7916.
14. Hegner, M., Smith, S. B. & Bustamante, C. (1999) Polymerisation and mechanical properties of single RecA-DNA filaments. *Proc. Natl. Acad. Sci.*, **96**, 10109.
15. Yin, H., Wang, M. D., Svoboda, K., Landick, R., Block, S. M. & Gelles, J. (1995) Transcription against an applied force. *Science*, **270**, 1653.
16. Wuite, G. J., Smith, S. B., Young, M., Keller, D. & Bustamante, C. (2000) Single molecule studies of the effect of template tension on T7 DNA polymerase activity. *Nature*, **404**, 103.

17. Davenport, J. R., Wuite, G. J., Landick, R. & Bustamante, C. (2000) Single-molecule study of transcriptional pausing and arrest by E. coli RNA polymerase. *Science*, **287**, 2497.

18. Strick T. R., Croquette, V. & Bensimon, D. (2000) Single-molecule analysis of DNA uncoiling by type II topoisomerase. *Nature*, **404**, 901.

19. Cui, Y. & Bustamante, C. (2000) Pulling a single chromatin fiber reveals the forces that maintain its higher-order structure. *Proc. Natl. Acad. Sci.*, **97**, 127.

20. Xia, Y. & Whitesides, G. M. (1998) Soft lithography. *Angew. Chem. Int. Ed.*, **37**, 550.

21. Ladoux, B & Doyle, P. S. (2000) Stretching tethered DNA chains in shear flow. *Europhys. Lett.*, **52**, 511.

22. Larson, R.G., Hu, H., Smith, D. E. & Chu, S. (1999) Brownian dynamics simulations of a DNA molecule in an extensional flow field, *J. Rheol.*, **43**, 267.

23. Doyle, P. S., Ladoux, B & Viovy, J-L. (2000) Dynamics of a tethered polymer in shear flow, *Phys. Rev. Lett.*, **84**, 4769.

24. Perkins, T. T., Smith, D.E, Larson, R. G.& Chu, S. (1995) Stretching of a single tethered polymer in an uniform flow. *Science*, **268**, 83.

25. Taylor, G. I. (1953) Dispersion of soluble matter in solvent flowing slowly through a tube, *Proc. R. Soc. London A*, **219**, 186.

26. Van Holde, K.E. (1988) In *Chromatin*. Springer-Verlag, New-York.

27. Luger, K., Mader, A.W., Richmond, R.K., Sargent, D. F. & Richmond, T. J. (1997) Crystal structure of the nucleosome core particle at 2.8 A resolution. *Nature*, **389**, 251.

28. Wolffe, A.P. (1998) *Chromatin structure and function*, 3rd edn, Academic Press, New York.

29. Ladoux, B., Quivy, J-P., Doyle, P. S., du Roure, O., Almouzni, G. & Viovy, J-L. (2000) Fast Kinetics of chromatin assembly revealed by single-molecule videomicroscopy and scanning force microscopy. *Proc. Natl. Acad. Sci.*, **97**, 14251.

30. Kaufman, P.D. & Almouzni, G. (2001) In *Chromatin Structure and Gene Expression: Frontiers in Molecular Biology*, 2nd edn, S. Elgin, J. Workman (eds), Oxford University Press.

31. Stein, A., Whitlock, J.P. Jr. & Bina, M. (1979) Acidic polypeptides can assemble both histones and chromatin in vitro at physiological ionic strength. *Proc. Natl. Acad. Sci.*, **76**, 5000.

32. Leuba, S.H., Yang, G., Robert, C., van Holde, K., Zlatanova, J. & Bustamante, C. (1994) Three-dimensional structure of extended chromatin fibres as revealed by tapping-mode scanning force microscopy. *Proc. Natl. Acad. Sci. USA*, **91**, 11621.